

*Erik Jonsson School of Engineering and Computer Science*

***Constricted Microfluidic Devices to Study the Effects  
of Transient High Shear Exposure on Platelets***

**UT Dallas Author(s):**

Trevor A. Snyder  
David W. Schmidtke

**Rights:**

©2017 American Institute of Physics

**Citation:**

Alsmadi, Nesreen Z., Sarah J. Shapiro, Christopher S. Lewis, Vinit M. Sheth, et al. 2017. "Constricted microfluidic devices to study the effects of transient high shear exposure on platelets." *Biomicrofluidics* 11(6), doi:10.1063/1.4989386

*This document is being made freely available by the Eugene McDermott Library of the University of Texas at Dallas with permission of the copyright owner. All rights are reserved under United States copyright law unless specified otherwise.*

## Constricted microfluidic devices to study the effects of transient high shear exposure on platelets

Nesreen Z. Alsmadi,<sup>1</sup> Sarah J. Shapiro,<sup>2</sup> Christopher S. Lewis,<sup>2</sup>  
 Vinit M. Sheth,<sup>1</sup> Trevor A. Snyder,<sup>3,4</sup> and David W. Schmidtke<sup>1,a)</sup>

<sup>1</sup>*Department of Bioengineering, University of Texas at Dallas, Richardson, Texas 75083, USA*

<sup>2</sup>*School of Chemical, Biological, and Materials Engineering, University of Oklahoma, Norman, Oklahoma 73019, USA*

<sup>3</sup>*INTEGRIS Advanced Cardiac Care, Nazih Zuhdi Transplant Institute, INTEGRIS Baptist Medical Center, Oklahoma City, Oklahoma 73112, USA*

<sup>4</sup>*VADovations, Inc., Oklahoma City, Oklahoma 73108, USA*

(Received 8 June 2017; accepted 2 November 2017; published online 28 November 2017)

Due to the critical roles that platelets play in thrombosis during many biological and pathological events, altered platelet function may be a key contributor to altered hemostasis, leading to both thrombotic and hemorrhagic complications. Platelet adhesion at arterial shear rates occurs through binding to von Willebrand Factor via the glycoprotein (GP) GPIb receptor. GPIb binding can induce platelet activation distinguishable by P-selectin (CD62P) surface expression and  $\alpha_{IIb}\beta_3$  activation, resulting in platelet aggregation and formation of the primary hemostatic plug to stop bleeding. Previous studies have used cone and plate viscometers to examine pathologic blood flow conditions, applied shear rates that are relatively low, and examined exposure times that are orders of magnitude longer compared to conditions present in ventricular assist devices, mechanical heart valves, or pathologic states such as stenotic arteries. Here, we evaluate the effect of short exposure to high shear on granule release and receptor shedding utilizing a constricted microfluidic device in conjunction with flow cytometry and enzyme-linked immunosorbent assay. In this study, platelets were first perfused through microfluidic channels capable of producing shear rates of 80 000–100 000 s<sup>-1</sup> for exposure times of 0–73 ms. We investigated platelet activation by measuring the expression level of CD62P (soluble and surface expressed), platelet factor 4 (PF4), and beta-thromboglobulin ( $\beta$ TG). In addition, we measured potential platelet receptor shedding of GPVI and GPIb using flow cytometry. The results showed that a single pass to high shear with short exposure times (milliseconds) had no effect on the levels of CD62P, GPVI and GPIb, or on the release of alpha granule content (PF4,  $\beta$ TG, and sP-selectin). *Published by AIP Publishing.* <https://doi.org/10.1063/1.4989386>

### I. INTRODUCTION

Accelerated blood flow conditions resulting in elevated shear stress levels occur commonly in pathologic cardiovascular diseases such as carotid or coronary arterial stenosis,<sup>1–5</sup> aortic valve stenosis,<sup>6–8</sup> and peripheral vascular disease.<sup>9</sup> Likewise, accelerated flow conditions are also frequently present in medical devices, including mechanical heart valves (MHVs),<sup>10,11</sup> ventricular assist devices (VADs),<sup>12</sup> and dialysis machines.<sup>13</sup> The impact of exposure of blood elements to elevated shear conditions remains incompletely investigated due to the challenges of re-creating extreme shear conditions, while not imposing non-physiologic exposure durations, inducing recirculation regions or stagnation zones creating artefactual activation, or stimulating thrombogenesis via materials and surface interactions. In addition, shear exposure can lead to a

<sup>a)</sup> Author to whom correspondence should be addressed: David.Schmidtke@utdallas.edu. Telephone: 972-883-5238.

panoply of responses including cellular destruction (lysis), platelet activation, platelet aggregation, and platelet receptor shedding, resulting in platelet dysfunction rather than activation.

Recent reports have investigated platelet activation and coagulation pathways in relation to possible injuries caused by the medical devices. For example, it has been reported that the high pathological shear rate produced within VADs causes von Willebrand Factor (vWF) multimer loss, platelet activation, and platelet receptor shedding, similar to the effects observed in stenosed aortic valves (Heyde's Syndrome).<sup>14–17</sup> Although many studies have investigated the effect of high shear on platelet responses, the vast majority have focused on lower levels of shear (less than  $10\,000\text{ s}^{-1}$ ) for long exposure times (minutes).<sup>14,17–21</sup> Most of these studies established a correlation between shear stress and exposure time to platelet activation and aggregation, yet only a few studies investigated the high shear and transient exposure times (less than 100 ms) encountered during blood passage through vascular conditions or present in VADs, MHVs, or other devices (Fig. 1).

Platelets play critical roles in hemostasis and thrombosis during many biological and pathological events. For example, when the sub-endothelium is exposed during injury, vWF multimers attach to the exposed collagen, which allows platelet adhesion to the immobilized vWF via the GPIb receptor.<sup>12,22–25</sup> Adhesion induces platelet activation distinguishable by higher expression levels of surface receptors GPIb, P-selectin, and  $\alpha_{\text{IIb}}\beta_3$ .<sup>26–28</sup> These receptors are involved in the initial attachment of the platelet to the vessel wall resulting in platelet aggregation and formation of the primary hemostatic plug to stop bleeding.<sup>26,29,30</sup> Hence, losing the high molecular weight vWF multimers and platelet receptors caused by non-physiological shear may contribute to the hemorrhagic propensity observed in VAD and Heyde Syndrome patients.<sup>11,12,31,32</sup>

Previous studies have shown that high shear rheologic conditions can cause platelet activation and vWF cleavage. Platelet activation was observed following repetitive high shear exposure,<sup>12,18,33</sup> but these conditions also induced receptor shedding<sup>16,17,21</sup> and/or leakage of intracellular materials.<sup>34,35</sup> Meyer *et al.* recognized that high shear conditions cause cleavage of high molecular weight vWF multimers, resulting in inadequate interaction between vWF and platelet GPIb receptors to initiate platelet-mediated thrombosis.<sup>36</sup> However, independent of the vWF and GPIb pathway, platelet activation by high shear appears to be regulated by the shear level and duration of shear exposure. For example, Hellums suggested that a defined shear stress magnitude threshold exists for platelet activation,<sup>37</sup> while chronic platelet activation and thromboembolic events observed in MHV patients have been attributed to high shear conditions.<sup>38</sup> Platelet GPIb and GPVI receptors were shed as a result of long exposure time to high shear.<sup>14,21</sup> Cone and plate viscometers have been employed for the majority of investigations of pathological flow conditions; however, the shear developed was typically orders of magnitude lower than the pathological conditions produced within arterial stenosis and cardiovascular medical devices.

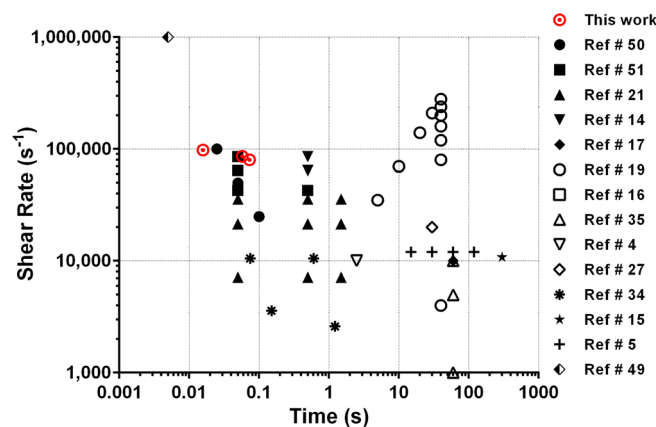


FIG. 1. Graphical representation of the previous literature studying the effect of shear on platelet activation and aggregation for time exposures of less than 300 s. Black color with a similar symbol represents data from the same paper.

The objective of this study was to develop an *in vitro* assay to evaluate the effect of physiological relevant time exposures ( $<75$  ms) to high shear on platelet granule release and receptor shedding utilizing microfluidics in conjunction with flow cytometry and enzyme-linked immunosorbent assay (ELISA). Platelets were first perfused through a microfluidic channel capable of producing a shear rate of  $80\,000$ – $100\,000\text{ s}^{-1}$  for exposure times of  $0$ – $73$  ms. Platelet degranulation was quantified by measuring the change in platelet expression of surface P-selectin, as well as soluble platelet granule release factors: P-selectin, Platelet factor 4 (PF4), and Beta-thromboglobulin ( $\beta$ TG). In addition, we also utilized flow cytometry to evaluate the decrease in surface expression (shedding) of platelet receptors GPVI and GPIb. In contrast to recent reports utilizing shearing devices with sub-optimal flow conditions, our results showed that short exposure times to high shear had no effect on the levels of platelet activation, platelet surface GPVI and GPIb, or on the release of alpha granule contents (PF4,  $\beta$ TG, and sP-selectin).

## II. METHODS

### A. Microfluidic device fabrication

Microfluidic shearing devices were designed to subject platelets to high shear and short exposure times. The channels had a narrow  $45\text{ }\mu\text{m}$  wide constriction that created a high shear region and areas of low shear upstream and downstream of the constriction (Table I). To vary the exposure time within the constriction, the constriction length was varied from  $11.6$  to  $46.2\text{ mm}$  (Table I). As a negative control, straight channel microfluidic devices with constant width ( $1500\text{ }\mu\text{m}$ ) and height ( $60\text{ }\mu\text{m}$ ) were fabricated with dimensions that generated shear rates matching those of the low shear regions of the constricted microfluidic devices.

To prepare microfluidic channels, a standard negative photolithography protocol was used with KMPR 1050 photoresist (MicroChem, Westborough, MA) fabricated on silicon wafers.<sup>39</sup> Briefly, a  $60\text{ }\mu\text{m}$  layer of photoresist was formed through spin coating followed by baking at  $100^\circ\text{C}$  for  $20$  min and then exposed to UV light at  $12\text{ mJ}/(\text{cm}^2\text{ s})$  for  $70$  s on an OmniCure<sup>TM</sup> Series 1000 Spot Curing. After exposure, the wafer was baked at  $100^\circ\text{C}$  for  $4$  min and placed in SU-8 Developer (MicroChem, Westborough, MA) for  $5$  min. The wafer then was coated with  $10\text{ }\mu\text{l}$  of (Tridecafluoro-1,1,2,2-TetraHydrooctyl) Methyl dichlorosilane for  $4$  h under vacuum.

Microfluidic channels were prepared from poly(dimethylsiloxane) (PDMS), using Sylgard<sup>®</sup> 184 Silicone Elastomer kits (Dow Corning Corporation; Midland, MI). To prepare the PDMS channels, the curing agent and base were thoroughly mixed in a  $1:10$  ratio, poured over the negative photolithography molds, and placed in a desiccator under vacuum for  $30$  min to remove air bubbles. After removal from the desiccator, elbow ports (Value Plastics Inc., Fort Collins, CO) were added

TABLE I. Comparative table of the dimensions and shear conditions for the different microfluidic channels utilized.  $L_c$  = length of constricted region;  $\dot{\epsilon}$  = elongation rate;  $t_{\text{exp}}$  = high shear exposure time; RDV = relative deviation in velocity; and NA = not applicable.

Channel type	$L_c$ (mm)	Wall shear rate ( $\text{s}^{-1}$ )	$\dot{\epsilon}$ ( $\text{s}^{-1}$ )	$t_{\text{exp}}$ (ms)	RDV (%)
Straight	NA	2500	NA	0	4.06
Constriction A	11.6	98 000	3930	16	1.06
Constriction B	38.6	86 000	3300	58	2.09
Constriction C	46.3	80 000	3100	73	0.20

as inlets for the channels. The PDMS was then placed in a drying oven at 80 °C for about 1 h. The channels were then removed from the mold, and an outlet port was cut into the PDMS.

## B. Fluid characterization of the microfluidic devices

Experimental determination of the velocity profiles in the constricted regions was accomplished by perfusing 1  $\mu\text{m}$  fluorescent beads (excitation/emission wavelength = 540/560 nm) through the microfluidic devices and performing microparticle image velocimetry ( $\mu\text{PIV}$ ) with a standard  $\mu\text{PIV}$  setup (TSI, Shoreview, MN). The system consisted of a Zeiss AxioObserver microscope equipped with a 40 $\times$  oil objective (NA = 1.4), a 16 MP PowerView camera, and a synchronization controller. A double pulsed Nd:YAG laser was employed as the illumination source. To map the velocity profile in the z-direction, PIV measurements were acquired at several z planes (0–50  $\mu\text{m}$  with a 5  $\mu\text{m}$  step size) and the velocities were determined using Insight4G software. Velocity profiles and wall shear rates were then subsequently created and calculated in Matlab. The theoretical velocity profile in the microfluidic channel was calculated using the Navier-Stokes for a rectangular channel<sup>40</sup>

$$v_x = \frac{16a^2}{\eta\pi^3} \left( -\frac{dp}{dx} \right) \sum_{i=1,3,5,\dots}^{\infty} (-1)^{(i-1)/2} \left[ 1 - \frac{\cosh(i\pi z/2a)}{\cosh(i\pi b/2a)} \right] \frac{\cos(i\pi y/2a)}{i^3}, \quad (1)$$

$$\dot{Q} = \frac{4ba^3}{3\eta} \left( -\frac{dp}{dx} \right) \left[ 1 - \frac{192a}{\pi^5 b} \sum_{i=1,3,5,\dots}^{\infty} \frac{\tanh(i\pi b/2a)}{i^5} \right], \quad (2)$$

with  $-a \leq y \leq a$  and  $-b \leq z \leq b$ .

The shear rate was calculated from a polynomial curve fit of the velocity versus z position from the wall.<sup>41</sup> High shear exposure times ( $t = L_c/v$ ) were calculated from the constriction length ( $L_c$ ) and mean linear fluid velocity ( $v$ ).<sup>42</sup> The relative deviation between the theoretical velocity value and experimental velocity data is defined as

$$\text{Relative Deviation} = \frac{(\text{Experimental velocity} - \text{Theoretical velocity})}{\text{Theoretical velocity}}. \quad (3)$$

The Reynolds number for the low shear and constricted regions was calculated by

$$Re = \frac{\rho Q D_h}{\mu A}, \quad (4)$$

where Q is the flow rate,  $D_h$  is the hydraulic diameter,  $\rho$  is the density of blood,  $\mu$  is the viscosity of blood, and A is the cross-sectional area of the channel.

The elongation rate in the constricted region was calculated from the change in the velocity over the distance as described previously<sup>43</sup>

$$\dot{\epsilon} = \frac{\Delta v}{D} = \frac{v_2 \left( 1 - \frac{w_2}{w_1} \right)}{D}$$

where  $v_2$  is the maximum velocity in the constriction,  $w_1$  is the width of the channel upstream of the constriction,  $w_2$  is the width of the channel in the constriction, and D is the distance over which the channel width changes.

## C. Blood collection

Blood was obtained via venipuncture from healthy adult volunteers and collected into sodium citrate vacutainers after informed consent was obtained according to methods approved by the University of Texas at Dallas Institutional Review Board (IRB). All donors

were self-reported free of medication and other health issues for two weeks prior to the blood draw. The first few milliliters of blood collected were discarded in a separate vacutainer to avoid activation associated with the blood draw.

#### D. Perfusion experiments

The microfluidic stamps were sealed to glass coverslips that were cleaned with a 28% solution of nitric acid for 1 h and then treated with 1% AquaSil siliconizing solution for 15 s. To create a permanent seal, the microfluidic stamps as well as the coverslips were treated in a PlasmaCleaner (Model PDC-32 G; Harrick; Ithaca, NY) for 1 min at the high power setting. One inch of silastic tubing (Dow Corning, Midland, MI) was then attached to the inlet elbows, and the other end of the tubing was connected to a Luer connector (Value Plastics; Fort Collins, CO), to enable connection to a syringe. The elbow was further sealed to the PDMS with epoxy. To prevent non-specific binding of blood cells, the channels were initially charged with a 0.5% solution of human serum albumin (HSA) in Hanks Buffered Salt Solution (HBSS) without calcium, magnesium, and phenol red (Corning cellgro<sup>®</sup>, Manassas, VA) and incubated for 30 min at room temperature. After 30 min, the channels were rinsed with HBSS. Blood samples were then infused into the channels at 80 000, 86 000, or 98 000 s<sup>-1</sup> and collected for flow cytometric analysis. Figure 2 shows a schematic diagram of the full procedure.

#### E. Flow cytometric analysis

To measure platelet activation and receptor levels following various shear exposures, the effluent from the microfluidic chambers was collected and analyzed via flow cytometry. 5  $\mu$ l of Alexa-488 conjugated anti-CD62P (anti-P-Selectin) was mixed with 100  $\mu$ l of HBSS, 5  $\mu$ l of anti-CD41a-PE (eBioscience, San Diego, CA), and 5  $\mu$ l of 20 mM GPRP (Anaspec, Fremont, CA) in a 1.7 ml micro-centrifuge tube. Finally, 5  $\mu$ l of the sheared and unsheared blood samples were added to each tube and incubated for 30 min. To evaluate whether transient exposure of platelets to high shear caused platelet receptor shedding, 5  $\mu$ l of anti-CD42b-FITC (eBioscience,

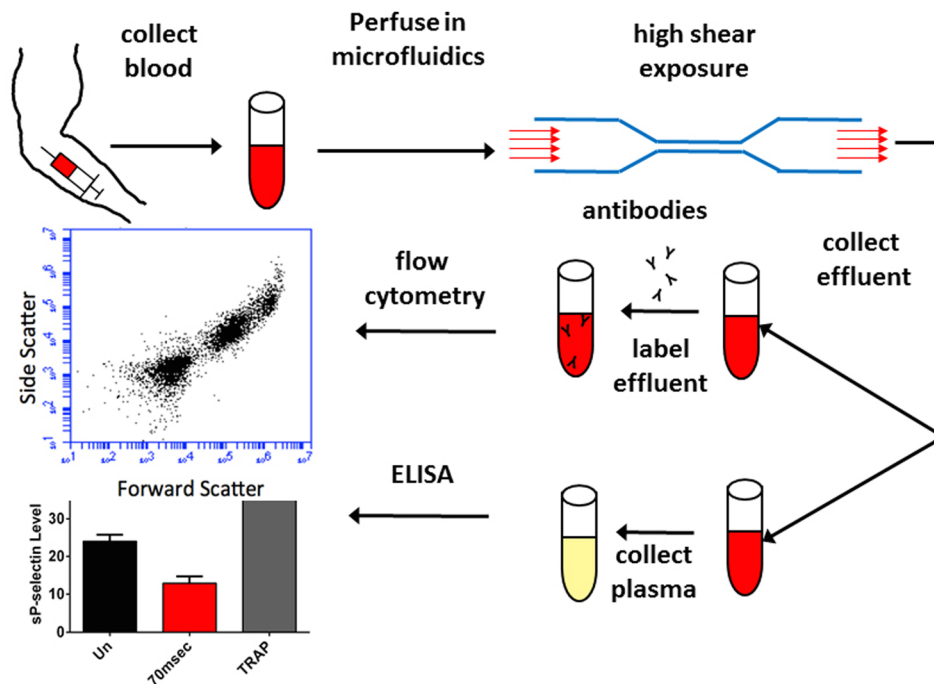


FIG. 2. Schematic diagram of the shearing experiment. Blood was perfused through constricted microfluidic channels to expose the platelets to shear rates ranging from 80 000–100 000 s<sup>-1</sup> and millisecond exposure times (16–73 ms). The effluent was then collected for either flow cytometry analysis or ELISA.

San Diego, CA), GPVI-eFluor<sup>®</sup>660 (eBioscience, San Diego, CA), or an isotype control was added. In some experiments, 5  $\mu$ l of 4 mg/ml TRAP-6 peptide (Bachem Biosciences, King of Prussia, PA) was added 5 min into the incubation period to promote platelet activation and serve as a positive control. Finally, 1 ml of HBSS was added to each tube after 25 min of incubation at room temperature. The cells were collected after 5 min of centrifugation at 1200 $\times$ g and then resuspended in 200  $\mu$ l of HBSS followed by 20  $\mu$ l of 16% paraformaldehyde (Electron Microscopy Sciences, Hatfield, PA). The samples were then run at slow acquisition speed on a BD Accuri<sup>™</sup> C6 flow cytometer (Franklin Lakes, NJ).

## F. Platelet count

To measure changes in the ratio of platelets to red blood cells (RBCs) in whole blood before and after perfusion through the microfluidic devices, 20  $\mu$ l of each sample was obtained from each condition and transferred to a 1.7 ml centrifuge tube containing 380  $\mu$ l of Hanks Buffered Salt Solution (HBSS) without calcium, magnesium, and phenol red. Then, 50  $\mu$ l of the diluted blood samples were placed into a 5 ml centrifuge tube with 2.5  $\mu$ l of anti-CD 41a-PE antibody (eBioscience, San Diego, CA) and 2.5  $\mu$ l of 20 mM GPRP (Anaspec, Fremont, CA). The samples were incubated for 30 min at room temperature. After 30 min of incubation, 2500  $\mu$ l of HBSS was added. The samples were then run at medium acquisition speed on a BD Accuri<sup>™</sup> C6 flow cytometer. Gates were set on the RBC and platelet clouds and allowed to collect 50 000 RBCs per shear condition.

## G. Detection of $\alpha$ granule release using Enzyme-linked immunosorbent assay (ELISA)

Blood samples from high shear (80 000–98 000 s<sup>-1</sup>), low shear (2500 s<sup>-1</sup>, straight channel devices), as well as unsheared and TRAP stimulated were centrifuged at 1200 $\times$ g for 5 min to remove cells. The plasma was then collected and kept at -20 °C until sample analysis. The ELISA assays for platelet factor 4 (PF4),  $\beta$  thromboglobulin ( $\beta$ TG), and soluble P-selectin (sP-selectin) were used according to the manufacturer's instructions (ABCAM, Inc., Boston, MA, USA). Briefly, for the PF4 ELISA assay (ABCAM Inc., ab189573), 50  $\mu$ l of a 1:1000 dilution of the plasma samples was added to a pre-coated 96 well plate. A 50  $\mu$ l capture and detection antibody cocktail was added to the samples and incubated for 45 min at room temperature on an orbital shaker. After 45 min, the solution was discarded and the plate was washed 3 times with 1 $\times$  washing buffer. On the last wash, the remaining washing buffer was removed by inverting the plate and blotting against a paper towel. Then, 100  $\mu$ l of TMB one-step substrate reagent was added to each well and incubated for 5 min at room temperature in the dark with vigorous shaking. After 5 min, 100  $\mu$ l of stop solution was added to each well. ELISA plates were read after 1 min of agitation at 450 nm using a microplate reader.

For measurement of  $\beta$ TG levels (ABCAM Inc., ab100613), 100  $\mu$ l at 1:4000 dilution of the plasma samples was added to a pre-coated 96 well plate and incubated for 2.5 h. After 2.5 h, the solution was discarded and the plate was washed 3 times as described above. A 100  $\mu$ l  $\beta$ TG 1 $\times$  biotinylated detection antibody was added to each well and incubated for 1 h at room temperature with gentle shaking. The solution was discarded, and the washing step was repeated. After washing the wells, a 100  $\mu$ l 1 $\times$  HRP-streptavidin solution was added to each well and incubated for 45 min at room temperature with gentle shaking. After 45 min, the solution was discarded and the plate was washed 3 times. Then, 100  $\mu$ l of TMB one-step substrate reagent was added to each well and incubated for 30 min at room temperature in the dark with gentle shaking. After 30 min, 50  $\mu$ l of stop solution was added to each well and the plate was read at 450 nm using a microplate reader. A similar procedure was used for sP-selectin ELISA (ABCAM Inc., ab100631) except the dilution factor was 1:1000 for each sample.

## H. Statistical analysis

When appropriate, statistical significance was assessed by one way ANOVA with a Tukey multiple comparison test, with  $P < 0.05$  considered as statistically significant.

### III. RESULTS AND DISCUSSION

#### A. Velocity profile

To determine the velocity profiles and wall shear rates inside the constricted region of the microfluidic devices, we acquired  $\mu$ PIV images at several  $z$  locations. For each  $Z$  plane, a velocity vector map was calculated using cross-correlation of image pairs. Figure 3(a) shows a representative time-average velocity vector map from 300 images with an exposure time of  $0.5\text{--}2\ \mu\text{s}$  using the  $\mu$ PIV technique for flow through a Type A constricted microfluidic channel.

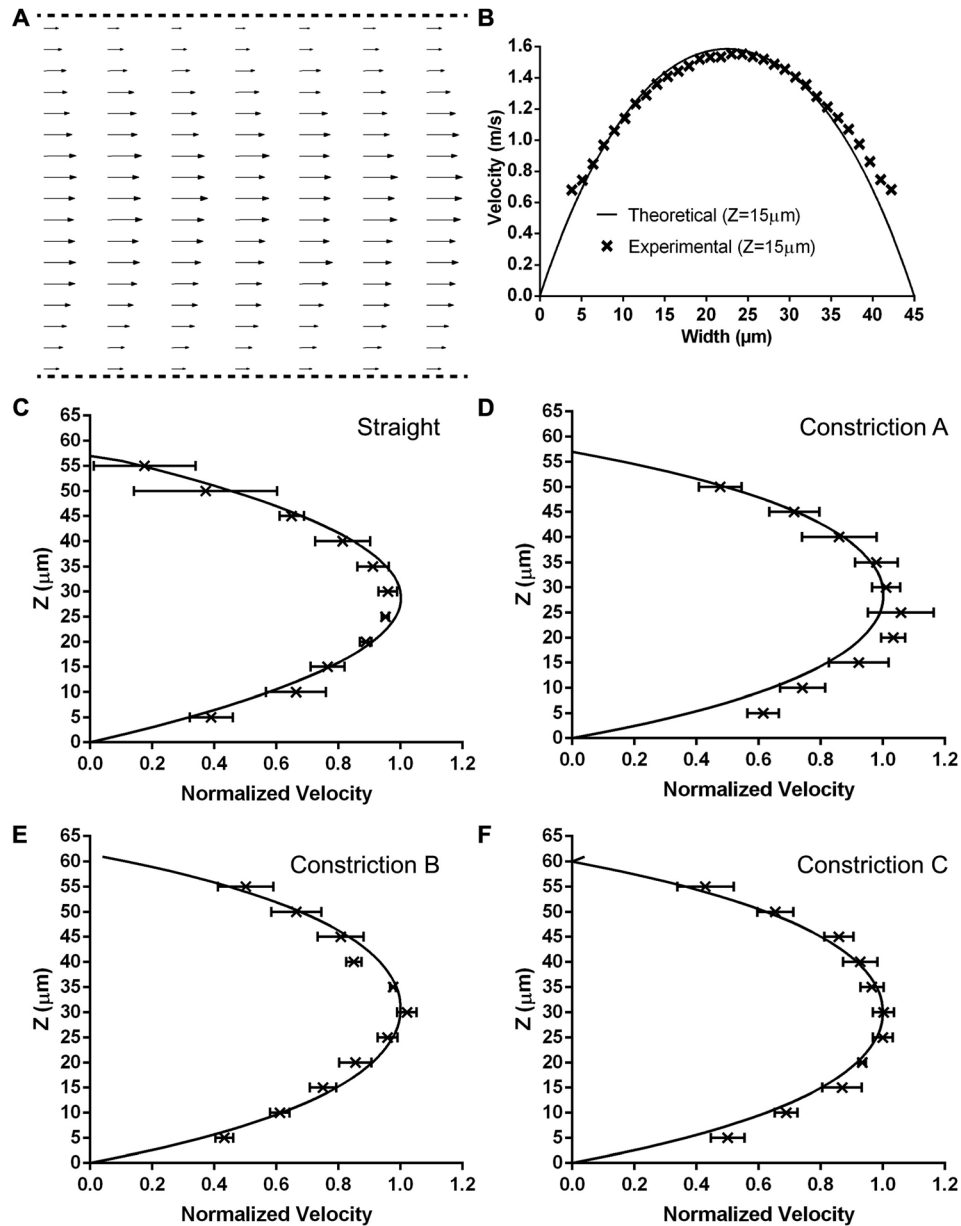


FIG. 3. Velocity profiles of the different microfluidic channels. (a) The measured velocity vectors in the  $x$ - $y$  position for a Type A constricted channel (shear rate =  $98\,000\ \text{s}^{-1}$  exposure time =  $16\ \text{ms}$ ). (b) Comparison of the experimental (x symbol) and theoretical (solid line) velocities at a height of  $15\ \mu\text{m}$ . The average, normalized velocity profiles with the  $Z$  position in comparison to the theoretical velocities (solid line) for a (c) straight channel, (d) Type A constricted channel, (e) Type B constricted channel, and (f) Type C constricted channel. The data represents the average of 3–5 experiments  $\pm$  standard deviation at each  $z$ -plane.

The flow profile in the constricted region exhibits a parabolic flow pattern with the maximum velocity vectors observed in the middle of the channel. To compare the experimental data with theoretical velocity profiles, we utilized a solution from the Navier-Stokes equation for a rectangular microchannel with a no-slip boundary condition at the wall. As shown in Fig. 3(b), there was a good agreement between the experimental and theoretical curves. We estimated the wall shear rate in the constricted region by making velocity measurements at several  $z$  planes and used a second order, polynomial curve fit.<sup>41,44</sup> Figures 3(c)–3(f) show a comparison between the experimental velocity profiles normalized with the theoretical velocity profile for the straight channel and the constricted channels of varying lengths. The error bars indicate the standard deviation at each  $z$ -plane for 3–5 experiments. Table I shows the calculated wall shear rates and exposure times for the different microfluidic channels. The accuracy of our results (2%) for the straight channel is comparable to the accuracy (3.6%) previously reported by Zheng and Silber-Li.<sup>45</sup>

## B. Millisecond exposure to high shear is insufficient to cause platelet activation

Previous studies have reported that exposure of platelets to high shear causes platelet activation.<sup>34,46–49</sup> However, a majority of these studies have involved shear rates less than  $20\,000\text{ s}^{-1}$  and exposure times of seconds to minutes. These results are problematic when considering what occurs during blood circulation. Even if a small percentage of platelets were activated during each passage through a MHV, VAD, or stenosed artery, nearly all platelets in the circulating blood would be activated in a few hours. This is because the entire blood volume circulates through the body about every minute, which is 60 times per hour or over 1400 times per day. Thus, we focused our efforts on investigating the effects of a single exposure to “pathologic” shear at physiologically relevant time durations. Little is known about the effects of sub-second exposure of platelets to high shear rates ( $60\,000$ – $100\,000\text{ s}^{-1}$ ) on platelet activation. To determine the platelet response to transient high shear exposure, whole blood was perfused through either high shear (i.e., constricted) or low shear (i.e., straight channel) microfluidic devices; the effluent was then collected and measured using flow cytometry. Figure 4 shows the measured levels of P-selectin positive platelets in sheared and unsheared blood samples.

When compared to unsheared blood samples, the flow cytometric measurement of overall P-selectin levels showed no significant increase in platelet activation following exposure of whole blood to a shear rate of  $98\,000\text{ s}^{-1}$  for 16 ms,  $86\,000\text{ s}^{-1}$  for 58 ms, and  $80\,000\text{ s}^{-1}$  for 73 ms in the constricted microfluidic channels. Similarly, there was minimal platelet activation

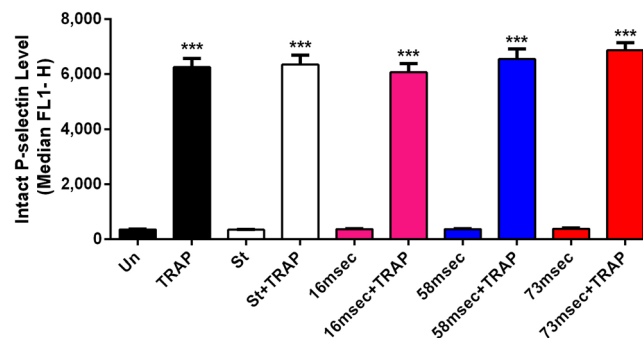


FIG. 4. Effect of transient high shear exposure on platelet P-selectin. Whole blood was perfused through the different constricted microfluidic channels, the effluent was collected and labeled with an Alexa-488 conjugated anti CD62P antibody or with an isotype-matched control mAb, and the expression level of P-selectin on the surface of platelets was analyzed by flow cytometry. To test the platelet reactivity following perfusion, some of the collected effluent from each device was incubated with TRAP. Levels. No significant difference in P-selectin expression was observed between the unsheared samples and the low shear (straight channel) or high shear samples. However, the level of P-selectin increased significantly after adding TRAP to the various matched samples. The data are presented as median  $\pm$  SEM and were derived from five to nine experiments collected in duplicate each time. Statistical significance was assessed by comparing each group to each other using a one-way ANOVA with a Tukey's multiple comparison test: \*\*\* $P < 0.0001$ .

upon exposure of platelets to  $2500\text{ s}^{-1}$  in straight microfluidic channels. In contrast, there was a 30-fold increase in P-selectin expression levels when unsheared blood samples were stimulated with TRAP-6 peptide (positive control). These results suggest that millisecond exposure of platelets to high shear is insufficient to cause platelet activation.

One possible cause for P-selectin levels to remain constant is the possibility that perfusion of the platelets through the microfluidic devices may cause rapid shedding of P-selectin and/or reduce their reactivity. To eliminate the possibility that high shear exposure reduced the reactivity of platelets, a separate set of experiments was performed in which whole blood was exposed to high shear rate conditions and the effluent was subsequently treated with TRAP-6 peptide (0.4 mg/ml). As shown in Fig. 4, treatment of platelets with TRAP-6 following shear exposure led to significant increases in both the surface expression levels of P-selectin and the number of P-selectin positive platelets ( $\sim 35\%$ ). Although there were differences in expression levels between donors, in each case there was a significant increase ( $p < 0.01$ ) in P-selectin expression in TRAP-6 activated samples compared to the negative controls. The P-selectin levels of shear exposed platelets were similar to unsheared blood treated with TRAP-6. These results with TRAP-6 provide evidence that microfluidic perfusion of platelets through the microfluidic devices at high shear did not cause platelets to lose their ability to activate.

A second possible cause for constant P-selectin levels in the microfluidic effluent is that activated platelets adhered to the device surfaces. To investigate this possibility, we used flow cytometry to measure changes in the ratio of platelets to red blood cells (RBCs) in whole blood before and after perfusion through the microfluidic devices. As shown in Fig. 5, there were no significant changes in the platelet:RBC ratio in any of the sheared microfluidic samples as compared to the unsheared whole blood sample. These results suggest that platelets did not adhere within the microfluidic device.

### C. Millisecond exposure of high shear did not cause platelet secretion of $\alpha$ -granules

The ability of platelets to store and release bioactive mediators upon activation allows platelets to play a major role in maintaining homeostasis after injury. To assess whether a millisecond exposure of high shear causes platelet release of the content of  $\alpha$ -granules, plasma PF4, sP-selectin, and  $\beta$ TG levels were measured using sandwich ELISA. When compared to unsheared blood samples, the overall sP-selectin levels showed no significant increase in platelet granule release following exposure of whole blood to a shear rate of  $98\,000\text{ s}^{-1}$  for 16 ms,  $86\,000\text{ s}^{-1}$  for 58 ms, and  $80\,000\text{ s}^{-1}$  for 73 ms in the constricted microfluidic channels. In contrast, there was a 2-fold increase in sP-selectin expression levels when unsheared blood samples were stimulated with TRAP-6 peptide [Fig. 6(a)]. Similarly, as can be seen in Figs. 6(b) and 6(c), levels of  $\beta$ TG (sCXCL7) and sPF4 did not increase after high shear exposure. However,

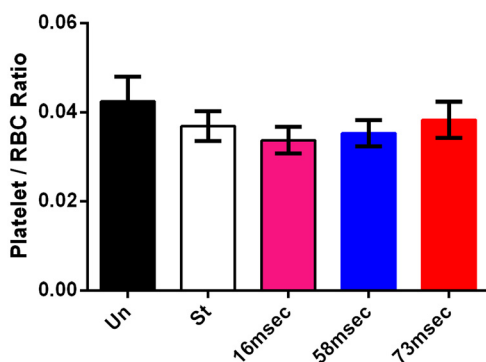


FIG. 5. Effect of high shear exposure on platelet counts. To determine whether platelets were being trapped within the microfluidic device, the ratio of platelets to red blood cells (RBCs) was analyzed by flow cytometry and used as a measure of platelet counts. No significant difference in the platelet:RBC ratio was observed between matching unsheared samples and the low shear (straight channel) or high shear samples. The number of cells is presented as the average value  $\pm$  SEM and was derived from four to six experiments.

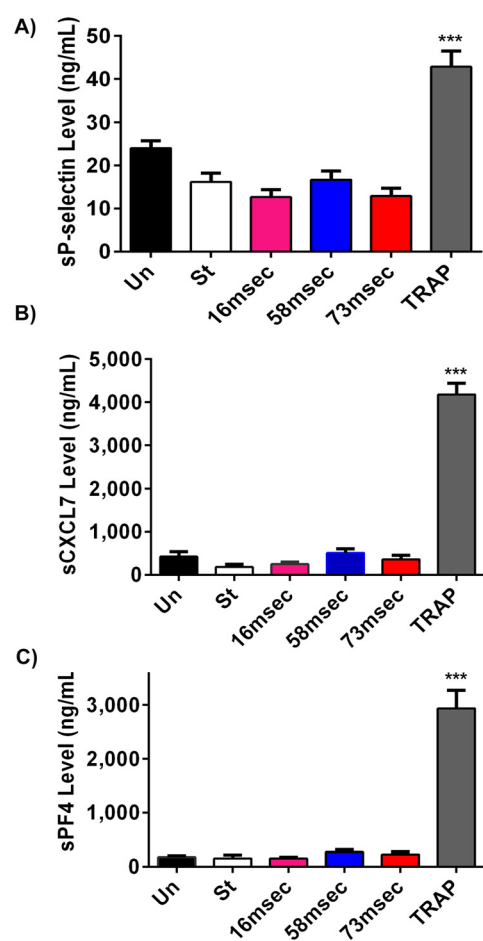


FIG. 6. Effect of high shear on platelet granule release. Whole blood was perfused through the constricted microfluidic devices, the effluents collected, and centrifuged to collect the plasma. The level of sP-selectin (a), sCXCL7 (b), and sPF4 (c) in the plasma samples was measured by ELISA. No significant difference in sP-selectin, sCXCL7, or sPF4 levels was observed between the unsheared samples and the low shear (straight channel) or high shear samples. However, treatment of the matched samples with TRAP showed a significant increase in the levels of SP-selectin, sCXCL7, and sPF4. The data are shown as the median value  $\pm$  SEM and are representative of 5–6 independent experiments with different donors. The statistical significance was assessed by comparing each group using one-way ANOVA with a Tukey's multiple comparison test: \* $P < 0.0001$ .

when unsheared samples were treated with TRAP-6, the levels of sCXCL7 and sPF4 increased 9.7- and 16-fold, respectively. These results further suggest that a millisecond exposure of platelets to high shear is insufficient to cause platelet degranulation.

#### D. Platelets do not shed GPIIb and GPIIb receptors after high shear rates for short exposure times

GPIIb receptors mediate platelet adhesion to von Willebrand factor under high arterial shear conditions, while GPIIb is an important platelet receptor for collagen binding. Since bleeding complications are reported in many VAD patients, investigators have examined the levels of GPIIb and GPIIb after high shear exposure. These previous studies show a clear reduction of GPIIb and GPIIb expression after high shear, at longer exposure time ( $\geq 0.5$  s). The degree of shedding observed was proportional to both the level of shear and the duration of time.<sup>14,15,17</sup> Although previous studies have reported shedding of GPIIb and GPIIb upon exposure of platelets to high shear for long duration (minutes), little is known about the effects of millisecond exposure on platelet receptor shedding. To evaluate the effect of transient high shear exposure on

GPIb and GPVI shedding, whole blood was infused through the constricted microfluidic devices. Exposing the platelets to a shear rate of  $98\,000\text{ s}^{-1}$  for 16 ms,  $86\,000\text{ s}^{-1}$  for 58 ms, and  $80\,000\text{ s}^{-1}$  for 73 ms did not lead to significant changes in the expression level of GPIb when compared to the unsheared platelets [Fig. 7(a)]. Likewise, Fig. 7(b) shows that there was no significant difference in GPVI levels after platelet exposure to a high shear when compared to the unsheared and low shear (i.e., straight channel) conditions. These results suggest that the millisecond exposure times to high shear are insufficient to cause platelet GPIb and GPVI receptor shedding. Furthermore, our results did not show a loss of GPIb and GPVI receptors on the platelet surface in contrast to previous reports which reported platelet receptor shedding in a Couette-shearing device.<sup>14,21</sup>

Our finding that transient high shear exposure did not cause platelet activation is in contrast to previous reports<sup>21,50,51</sup> which suggested that platelet activation was observed after a shear exposure of  $1000\text{ dyne/cm}^2$  ( $100\,000\text{ s}^{-1}$ ) for 25 ms and 300 Pa ( $85\,714\text{ s}^{-1}$ ) for 50 ms. We suspect that the lack of agreement in these studies is due to differences in the shearing device design, experimental protocol, and parameters measured to assess platelet activation. For example, in the paper by Sheriff *et al.*,<sup>50</sup> platelet activation was measured in isolated platelet solutions with hypercalcemic conditions and did not passivate the test loop surfaces to avoid platelet deposition. The advantage of using whole blood is that there is less manipulation of the sample, which should reduce the likelihood of artefactual activation of the platelets. Another experimental difference between the studies is that they used a syringe capillary viscometer to generate the shear levels, while we employed a constricted microfluidic device capable of producing a range of shear rates and exposure times utilizing microliters of blood. A final difference is that they measured the platelet activation level using a prothrombinase assay, which is

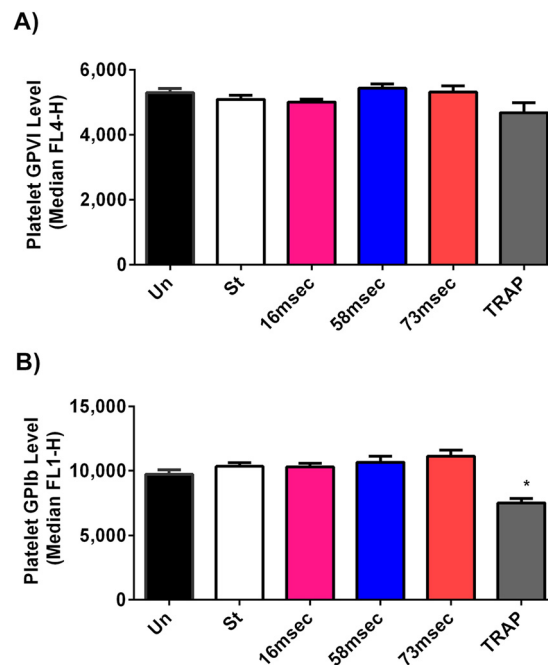


FIG. 7. Effect of transient high shear exposure on surface levels of GPVI and GPIb. Whole Blood was perfused through the different constricted microfluidic channels, the effluent was collected and labeled with an anti-GPIb antibody (anti-CD42b-FITC), an anti-GPVI antibody (GPVI-eFluor®660), or an isotype-matched control mAb, and the expression levels of GPIb and GPVI on the surface of platelets were analyzed by flow cytometry. (a) No significant difference in the surface expression levels of GPVI was observed between the unsheared, low shear, high shear, and TRAP-treated samples. (b) No significant difference in the surface expression levels of GPIb was observed between the unsheared, low shear, and high shear samples. Treatment of the unsheared sample with TRAP led to a significant decrease in the surface expression of GPIb. The data are shown as the median value  $\pm$  SEM and were derived from five to nine repeated experiments with duplicates each time, giving similar results. The statistical significance was assessed by comparing each group to each other using one-way ANOVA with a Tukey's multiple comparison test: \* $P < 0.05$  considered significance.

an indirect measurement of the catalytic function of the platelet membrane following activation, primarily due to phosphatidyl serine exposure.<sup>52</sup> We measured surface receptors (P-selectin, GPIb, and GPVI) and granule release constituents (PF4 and  $\beta$ TG) to examine both platelet activation and potential shear-induced platelet dysfunction.

Differences in the flow patterns between the studies could also explain the differences in platelet activation observed. In the report by Ding *et al.*,<sup>51</sup> whole blood samples were sheared in modified blood pumps as Couette shearing devices, each of which have limitations. A Hemolyzer-H device used mechanical pin bearings which generate high shear, heat, and create recirculation zones, both pre- and post-exposure to the actual high shear test region. Convergence of a rotating cone produces large recirculation regions immediately upstream of the constricted shear gap. The Hemolyzer-L device uses a magnetic bearing, which results in retrograde flow through the bearing gaps. Previous studies have suggested that the entrapment of platelets in a recirculation zone increases the exposure time (albeit at a lower shear stress level) and contact time with the device walls, both of which can lead to platelet activation.<sup>53–55</sup>

In support of the importance of flow pattern differences, Ha and Lee<sup>56</sup> reported that platelets became aggregated in the post-constriction region of a constricted microfluidic channel where recirculation and stagnation flow regions were present. At low flow rates ( $Re < 5.4$ ), no flow separation or recirculation zones were observed in the post-constriction region, while as the flow rate was increased ( $Re = 6.7$  to  $13.4$ ), significant recirculation zones developed and platelet aggregation was observed. To compare our results, we also calculated the Reynolds number and determined it to be  $Re = 0.81$  for a flow rate of  $125 \mu\text{l}/\text{min}$ . This value was well below the  $Re$  values observed to cause recirculation zones. To confirm these results, we also imaged the post-constriction region of our devices when whole blood was perfused. As blood exited the constricted region and replaced the buffer present in the channel, we observed streak lines that were parallel to the microfluidic wall (Fig. 8, Multimedia view). The streak lines observed in Fig. 8 were due to the blood cells traveling faster than the speed of the camera. Initially, we observed a cell free region near the channel wall. However, this cell-free layer decreased rapidly within 10 s, and subsequently, the streak lines remained parallel to the channel wall. The observation that the streak lines were parallel to the channel wall suggests that

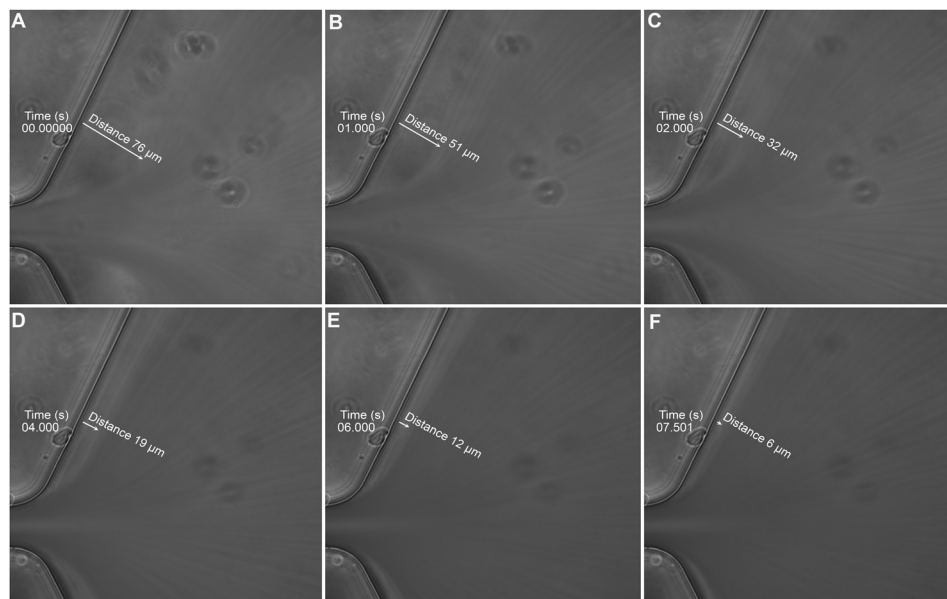


FIG. 8. Development of the blood flow pattern in the post-constriction region. Digitized images taken from a video sequence of the flow patterns that develop in the post-constriction region when blood was initially perfused through a Type A constricted channel at  $125 \mu\text{l}/\text{min}$  ( $Re = 0.8$ ). The white arrows provide an estimate of the thickness of the cell free layer that is present near the microchannel wall. Multimedia view: <https://doi.org/10.1063/1.4989386.1>

there were no recirculation zones or platelet aggregation in the post-constriction region of our devices.

#### IV. CONCLUSIONS

In this study, we describe a simple design of a microfluidic device capable of producing very high, non-physiological shear rates for millisecond exposure time. This technique has the advantages of providing a well-controlled range of shears and exposure times without recirculation zones. In addition, the microfluidic design presents an advantage over traditional shearing devices by utilizing microliter sample volumes. We demonstrated here that a single transient exposure (16–73 ms) of platelets to high shear rates ( $80\,000\text{--}100\,000\text{ s}^{-1}$ ) was insufficient to induce platelet activation, granule release, and receptor shedding. These shear conditions mimic those in blood contacting devices such as VADs or MHVs. We also demonstrated that the reactivity of platelets was not impaired by the high shear exposure.

Although our system can mimic several aspects of the high shear conditions present in VADs, it does have some limitations when compared to the *in vivo* situation. One limitation of our system is that the rectangular geometry of the microchannels will affect the normal margination of cells that occurs in circular microvessels present *in vivo*. A second limitation of our system is that it only allows for a single exposure to high shear, while *in vivo* platelets can be exposed to high shear during each pass through the VAD. Future designs will include multiple passes through the device to more closely mimic the repeated high shear exposures, which occur during blood circulation. Despite these limitations, this experimental platform allows researchers to study the response of blood cells (e.g., platelets and leukocytes) to transient high shear exposure present in medical devices and pathologic cardiovascular diseases.

#### ACKNOWLEDGMENTS

Research reported in this publication was supported by the National Heart, Lung, And Blood Institute of the National Institutes of Health under Award Number R21HL115601 and R21HL132286. The content is solely the responsibility of the authors and does not necessarily represent the official views of the National Institutes of Health.

- <sup>1</sup>F. D. Kolodgie, K. Yahagi, H. Mori, M. E. Romero, H. H. Trout, A. V. Finn, and R. Virmani, "High-risk carotid plaque: Lessons learned from histopathology," *Semin. Vasc. Surg.* **30**(1), 31–43 (2017).
- <sup>2</sup>D. Mozaffarian, E. J. Benjamin, A. S. Go, D. K. Arnett, M. J. Blaha, M. Cushman, S. R. Das, S. De Ferranti, J. P. Després, H. J. Fullerton, *et al.*, "Heart disease and stroke statistics-2016 update—A report from the American Heart Association," *Circulation* **133**, e38 (2016).
- <sup>3</sup>S. Goto, H. Sakai, M. Goto, M. Ono, Y. Ikeda, S. Handa, and Z. M. Ruggeri, "Enhanced shear-induced platelet aggregation in acute myocardial infarction," *Circulation* **99**(5), 608–613 (1999).
- <sup>4</sup>J. N. Zhang, A. L. Bergeron, Q. Yu, C. Sun, L. V. McIntire, J. A. López, and J. F. Dong, "Platelet aggregation and activation under complex patterns of shear stress," *Thromb. Haemostasis* **88**(5), 817–821 (2002).
- <sup>5</sup>S. G. Kamat, A. D. Michelson, S. E. Benoit, J. L. Moake, D. Rajasekhar, J. D. Hellums, M. H. Kroll, and A. I. Schafer, "Fibrinolysis inhibits shear stress-induced platelet aggregation," *Circulation* **92**(6), 1399–1407 (1995).
- <sup>6</sup>S. Pasta, A. Rinaudo, A. Luca, M. Pilato, C. Scardulla, T. G. Gleason, and D. A. Vorp, "Difference in hemodynamic and wall stress of ascending thoracic aortic aneurysms with bicuspid and tricuspid aortic valve," *J. Biomech.* **46**(10), 1729–1738 (2013).
- <sup>7</sup>F. Von Knobelsdorff-Brenkenhoff, A. Karunaharamoorthy, R. F. Trauzeddel, A. J. Barker, E. Blaszczyk, M. Markl, and J. Schulz-Menger, "Evaluation of aortic blood flow and wall shear stress in aortic stenosis and its association with left ventricular remodeling," *Circ. Cardiovasc. Imaging* **9**(3), e004038 (2016).
- <sup>8</sup>N. Saikrishnan, L. Mirabella, and A. P. Yoganathan, "Bicuspid aortic valves are associated with increased wall and turbulence shear stress levels compared to trileaflet aortic valves," *Biomech. Model Mechanobiol.* **14**(3), 577–588 (2015).
- <sup>9</sup>M. H. Kroll, J. D. Hellums, L. V. McIntire, A. I. Schafer, and J. L. Moake, "Platelets and shear stress," *Blood* **88**(5), 1525–1541 (1996).
- <sup>10</sup>J. T. Ellis, B. R. Travis, and A. P. Yoganathan, "An *in vitro* study of the hinge and near-field forward flow dynamics of the St. Jude Medical<sup>®</sup> Regent<sup>™</sup> Bileaflet mechanical heart valve," *Ann. Biomed. Eng.* **28**(5), 524–532 (2000).
- <sup>11</sup>D. Bluestein, "Research approaches for studying flow-induced thromboembolic complications in blood recirculating devices," *Expert Rev. Med. Devices* **1**(1), 65–80 (2004).
- <sup>12</sup>K. H. Fraser, T. Zhang, M. E. Taskin, B. P. Griffith, and Z. J. Wu, "A quantitative comparison of mechanical blood damage parameters in rotary ventricular assist devices: shear stress, exposure time and hemolysis index," *J. Biomech. Eng.* **134**(8), 81002 (2012).
- <sup>13</sup>H. T. Spijker, R. Graaff, P. W. Boonstra, H. J. Busscher, and W. Van Oeveren, "On the influence of flow conditions and wettability on blood material interactions," *Biomaterials* **24**(26), 4717–4727 (2003).

- <sup>14</sup>Z. Chen, N. K. Mondal, J. Ding, J. Gao, B. P. Griffith, and Z. J. Wu, "Shear-induced platelet receptor shedding by non-physiological high shear stress with short exposure time: Glycoprotein Ib $\alpha$  and Glycoprotein VI," *Thromb. Res.* **135**(4), 692–698 (2015).
- <sup>15</sup>Y. Miyazaki, S. Nomura, T. Miyake, H. Kagawa, C. Kitada, H. Taniguchi, Y. Komiyama, Y. Fujimura, Y. Ikeda, and S. Fukuhara, "High shear stress can initiate both platelet aggregation and shedding of procoagulant containing microparticles," *Blood* **88**(9), 3456–3464 (1996).
- <sup>16</sup>H. Cheng, R. Yan, S. Li, Y. Yuan, J. Liu, C. Ruan, and K. Dai, "Shear-induced interaction of platelets with von Willebrand factor results in glycoprotein Iba $\alpha$  shedding," *Am. J. Physiol. - Hear. Circ. Physiol.* **297**(6), H2128–H2135 (2009).
- <sup>17</sup>M. Al-Tamimi, C. W. Tan, J. Qiao, G. J. Pennings, A. Javazadegan, A. S. C. Yong, J. F. Arthur, A. K. Davis, J. Jing, F. T. Mu *et al.*, "Pathologic shear triggers shedding of vascular receptors: A novel mechanism for down-regulation of platelet glycoprotein VI in stenosed coronary vessels," *Blood* **119**(18), 4311–4320 (2012).
- <sup>18</sup>J. Sheriff, J. S. Soares, M. Xenos, J. Jesty, and D. Bluestein, "Evaluation of shear-induced platelet activation models under constant and dynamic shear stress loading conditions relevant to devices," *Ann. Biomed. Eng.* **41**(6), 1279–1296 (2013).
- <sup>19</sup>J. Sheriff, D. Bluestein, G. Girdhar, and J. Jesty, "High-shear stress sensitizes platelets to subsequent low-shear conditions," *Ann. Biomed. Eng.* **38**(4), 1442–1450 (2010).
- <sup>20</sup>D. A. Rubenstein and W. Yin, "Quantifying the effects of shear stress and shear exposure duration regulation on flow induced platelet activation and aggregation," *J. Thromb. Thrombolysis* **30**(1), 36–45 (2010).
- <sup>21</sup>Z. Chen, N. K. Mondal, J. Ding, S. C. Koenig, M. S. Slaughter, B. P. Griffith, and Z. J. Wu, "Activation and shedding of platelet glycoprotein IIb/IIIa under non-physiological shear stress," *Mol. Cell. Biochem.* **409**(1–2), 93–101 (2015).
- <sup>22</sup>Y. Hori, M. Hayakawa, A. Isonishi, K. Soejima, M. Matsumoto, and Y. Fujimura, "ADAMTS13 unbound to larger von Willebrand factor multimers in cryosupernatant: implications for selection of plasma preparations for thrombotic thrombocytopenic purpura treatment," *Transfusion* **53**(12), 3192–3202 (2013).
- <sup>23</sup>U. Geisen, C. Heilmann, F. Beyersdorf, C. Benk, M. Berchtold-Herz, C. Schlensak, U. Budde, and B. Zieger, "Non-surgical bleeding in patients with ventricular assist devices could be explained by acquired von willebrand disease," *Eur. J. Cardio-thoracic Surg.* **33**(4), 679–684 (2008).
- <sup>24</sup>C. Heilmann, U. Geisen, F. Beyersdorf, L. Nakamura, C. Benk, M. Berchtold-Herz, G. Trummer, C. Schlensak, and B. Zieger, "Acquired von Willebrand syndrome in patients with ventricular assist device or total artificial heart," *Thromb. Haemost.* **103**(5), 962–967 (2010).
- <sup>25</sup>C. Heilmann, U. Geisen, F. Beyersdorf, L. Nakamura, C. Benk, G. Trummer, M. Berchtold-Herz, C. Schlensak, and B. Zieger, "Acquired von Willebrand syndrome in patients with extracorporeal life support (ECLS)," *Intensive Care Med.* **38**(1), 62–68 (2012).
- <sup>26</sup>D. Varga-Szabo, I. Pleines, and B. Nieswandt, "Cell adhesion mechanisms in platelets," *Arterioscler., Thromb., Vasc. Biol.* **28**(3), 403–412 (2008).
- <sup>27</sup>M. Merten, T. Chow, J. D. Hellums, and P. Thiagarajan, "A new role for P-selectin in shear-induced platelet aggregation," *Circulation* **102**(17), 2045–2050 (2000).
- <sup>28</sup>S. S. Smyth, R. P. McEver, A. S. Weyrich, C. N. Morrell, M. R. Hoffman, G. M. Arepally, P. A. French, H. L. Dauerman, R. C. Becker, and 2009 Platelet Colloquium Participants, "Platelet functions beyond hemostasis," *J. Thromb. Haemost.* **7**(11), 1759–1766 (2009).
- <sup>29</sup>S. P. Jackson, "The growing complexity of platelet aggregation," *Blood* **109**(12), 5087–5095 (2007).
- <sup>30</sup>A. J. Reininger, "Platelet function under high shear conditions," *Hamostaseologie* **29**(1), 21–24 (2009).
- <sup>31</sup>R. J. Gordon, A. D. Weinberg, F. D. Pagani, M. S. Slaughter, P. S. Pappas, Y. Naka, D. J. Goldstein, W. P. Dembitsky, J. C. Giacalone, J. Ferrante *et al.*, "Prospective, multicenter study of ventricular assist device infections," *Circulation* **127**(6), 691–702 (2013).
- <sup>32</sup>B. Thamsen, B. Blümel, J. Schaller, C. O. Paschereit, K. Affeld, L. Goubergrits, and U. Kertzscher, "Numerical analysis of blood damage potential of the HeartMate II and HeartWare HVAD rotary blood pumps," *Artif. Organs* **39**(8), 651–659 (2015).
- <sup>33</sup>M. Nobili, J. Sheriff, U. Morbiducci, A. Redaelli, and D. Bluestein, "Platelet activation due to hemodynamic shear stresses: damage accumulation model and comparison to *in vitro* measurements," *ASAIO J.* **54**(1), 64–72 (2008).
- <sup>34</sup>P. A. Holme, U. Orvim, M. J. Hamers, N. O. Solum, F. R. Brosstad, R. M. Barstad, and K. S. Sakariassen, "Shear-induced platelet activation and platelet microparticle formation at blood flow conditions as in arteries with a severe stenosis," *Arterioscler. Thromb. Vasc. Biol.* **17**(4), 646–653 (1997).
- <sup>35</sup>J. H. Haga, S. M. Slack, and L. K. Jennings, "Comparison of shear stress-induced platelet microparticle formation and phosphatidylserine expression in presence of alphaIIb $\beta$ 3 antagonists," *J. Cardiovasc. Pharmacol.* **41**(3), 363–371 (2003).
- <sup>36</sup>A. L. Meyer, D. Malehsa, C. Bara, U. Budde, M. S. Slaughter, A. Haverich, and M. Strueber, "Acquired von Willebrand syndrome in patients with an axial flow left ventricular assist device," *Circ.: Heart Failure* **3**(6), 675–681 (2010).
- <sup>37</sup>J. D. Hellums, "1993 Whitaker Lecture: Biorheology in thrombosis research," *Ann. Biomed. Eng.* **22**(5), 445–455 (1994).
- <sup>38</sup>E. G. Butchart, A. Ionescu, N. Payne, J. Giddings, G. L. Grunkemeier, and A. G. Fraser, "A new scoring system to determine thromboembolic risk after heart valve replacement," *Circulation* **108**(Suppl 1), II-68–II-74 (2003).
- <sup>39</sup>E. A. Shimp, N. Z. Alsmadi, T. Cheng, K. H. Lam, C. S. Lewis, and D. W. Schmidtke, "Effects of shear on P-Selectin deposition in microfluidic channels," *Biomicrofluidics* **10**(2), 024128 (2016).
- <sup>40</sup>N. Nguyen and S. Wereley, *Fundamentals and Applications of Microfluidics* (Artech House, 2006).
- <sup>41</sup>S. W. Stone, C. D. Meinhardt, and S. T. Wereley, "A microfluidic-based nanoscope," *Exp. Fluids* **33**(5), 613–619 (2002).
- <sup>42</sup>H. L. Goldsmith, D. N. Bell, S. Braovac, A. Steinberg, and F. McIntosh, "Physical and chemical effects of red cells in the shear-induced aggregation of human platelets," *Biophys. J.* **69**(4), 1584–1595 (1995).
- <sup>43</sup>C. E. Sing and A. Alexander-Katz, "Elongational flow induces the unfolding of von willebrand factor at physiological flow rates," *Biophys. J.* **98**, L35–L37 (2010).
- <sup>44</sup>C. D. Meinhardt, S. T. Wereley, and J. G. Santiago, "PIV Measurements of a Microchannel Flow," *Exp. Fluids* **27**(5), 414–419 (1999).

- <sup>45</sup>X. Zheng and Z. H. Silber-Li, "Measurement of velocity profiles in a rectangular microchannel with aspect ratio  $\alpha = 0.35$ ," *Exp. Fluids* **44**(6), 951–959 (2008).
- <sup>46</sup>C. Baldauf, R. Schneppenheim, W. Stacklies, T. Obser, A. Pieconka, S. Schneppenheim, U. Budde, J. Zhou, and F. Gräter, "Shear-induced unfolding activates von Willebrand factor A2 domain for proteolysis," *J. Thromb. Haemostasis* **7**(12), 2096–2105 (2009).
- <sup>47</sup>T. Kragh, M. Napoleone, M. A. Fallah, H. Gritsch, M. F. Schneider, and A. J. Reininger, "High shear dependent von willebrand factor self-assembly fostered by platelet interaction and controlled by ADAMTS13," *Thromb. Res.* **133**(6), 1079–1087 (2014).
- <sup>48</sup>K. B. Neeves, S. F. Maloney, K. P. Fong, A. A. Schmaier, M. L. Kahn, L. F. Brass, and S. L. Diamond, "Microfluidic focal thrombosis model for measuring murine platelet deposition and stability: PAR4 signaling enhances shear-resistance of platelet aggregates," *J. Thromb. Haemostasis* **6**(12), 2193–2201 (2008).
- <sup>49</sup>G. Colantuoni, J. D. Hellums, J. L. Moake, and C. P. J. Alfery, "The response of human platelets to shear stress at short exposure times," *Trans. Am. Soc. Artif. Intern. Organs* **23**, 626–631 (1977).
- <sup>50</sup>J. Sheriff, P. L. Tran, M. Hutchinson, T. DeCook, M. J. Slepian, and D. Bluestein, "Repetitive hypershear activates and sensitizes platelets in a dose-dependent manner," *Artif. Organs* **40**(6), 586–595 (2016).
- <sup>51</sup>J. Ding, Z. Chen, S. Niu, J. Zhang, N. K. Mondal, B. P. Griffith, and Z. J. Wu, "Quantification of shear-induced platelet activation: High shear stresses for short exposure time," *Artif. Organs* **39**(7), 576–583 (2015).
- <sup>52</sup>M. Mazepa, M. Hoffman, and D. Monroe, "Superactivated platelets: Thrombus regulators, thrombin generators, and potential clinical targets," *Arterioscler., Thromb., Vasc. Biol.* **33**(8), 1747–1752 (2013).
- <sup>53</sup>S. Raz, S. Einav, Y. Alemu, and D. Bluestein, "Platelet activation in flow through a stenosis model: Comparison between CFD and CDPIV Results," in *Proceedings of the Second Joint EMBS/BMES Conference, Houston, TX* (2002), pp. 901–902.
- <sup>54</sup>H. A. Simon, L. P. Dasi, H. L. Leo, and A. P. Yoganathan, "Spatio-temporal flow analysis in bileaflet heart valve hinge regions: Potential analysis for blood element damage," *Ann. Biomed. Eng.* **35**(8), 1333–1346 (2007).
- <sup>55</sup>J. M. Jiménez, V. Prasad, M. D. Yu, C. P. Kampmeyer, A. H. Kaakour, P. J. Wang, S. F. Maloney, N. Wright, I. Johnston, Y. Z. Jiang, and P. F. Davies, "Macro- and microscale variables regulate stent haemodynamics, fibrin deposition and thrombomodulin expression," *J. R. Soc. Interface* **11**(94), 20131079 (2014).
- <sup>56</sup>H. Ha and S. J. Lee, "Hemodynamic features and platelet aggregation in a stenosed microchannel," *Microvasc. Res.* **90**, 96–105 (2013).